# Electronic *d*-band properties of gold nanoclusters grown on amorphous carbon

Anton Visikovskiy,[1,*] Hisashi Matsumoto,[1] Kei Mitsuhara,[1] Toshitaka Nakada,[1] Tomoki Akita,[2] and Yoshiaki Kido[1]

[1]*Department of Physics, Ritsumeikan University, Kusatsu, Shiga 525-8577, Japan*

[2]*Advanced Industrial Science and Technology (AIST) Kansai Center, Ikeda, Osaka 563-8577, Japan*

(Received 13 September 2010; revised manuscript received 3 February 2011; published 20 April 2011)

The electronic *d*-band properties are important factors for the emerging catalytic activity of Au nanoclusters of sub-5-nm size. We analyzed the *d*-band properties of Au nanoclusters grown on amorphous carbon supports by photoelectron spectroscopy using synchrotron-radiation light coupled with high-resolution ion scattering spectrometry which enables us to estimate the size and shape of Au nanoclusters. The *d*-band width ($W_d$), *d*-band center position ($E_d$), and apparent $5d_{3/2}$-$d_{5/2}$ spin-orbit splitting ($E_{SO}$) were determined as a function of a number of Au atoms per cluster ($n_A$) and an average coordination number ($n_C$) in a wide range ($11 < n_A < 1600$). The $W_d$ and $E_{SO}$ values decrease steeply with decreasing $n_A$ below ~150 owing to band narrowing which is caused by hybridization of fewer wave functions of the valence electrons. However, $E_d$ shifts to the higher binding energy side with decreasing cluster size. The rapid movement of $E_d$ is attributed to the dynamic final-state effect, which results in higher binding energy shifts of core and valence states due to a positive hole created after photoelectron emission. We have estimated the contribution from the final-state effect and derived the approximated initial-state spectra. Modified data, however, still show a slight movement of the *d*-band center away from the Fermi level ($E_F$) although the $E_d$ values for Au nanoclusters are closer to $E_F$ compared to the bulk value. This behavior is ascribed to the contraction of average Au-Au bond length with decreasing cluster size.

DOI: 10.1103/PhysRevB.83.165428 PACS number(s): 73.22.−f, 82.45.Jn, 82.80.Pv, 34.50.−s

## I. INTRODUCTION

Gold (Au) is recognized as the most inert metal of the Periodic Table.[1,2] It is the only metal which does not form any stable oxides under normal conditions. The extreme inertness of Au is attributed to its electronic structure, especially the structure of the *d* band, its width ($W_d$), and position (usually given by the *d*-band center parameter $E_d$).[2] The difference in the properties of the other noble metals is also attributed to this effect. Two decades ago Haruta *et al.*[3,4] found that the catalytic activity of Au nanoclusters dramatically increases if the cluster size becomes smaller than ~5 nm. Since then many efforts have been devoted to clarifying the mechanism of the catalytic activity of sub-5-nm Au clusters. As probable factors, the following points have been discussed so far: (i) the effect of the metal-insulator transition,[5] (ii) charge transfer between the nanoparticle and support,[6,7] and (iii) the support-mediated strain effect.[8] All of these effects certainly contribute to the catalytic activities of Au nanoclusters; however, it has been shown that the most drastic changes in the catalytic activity can be attributed to changes in the size and shape of Au nanoclusters.[9–11] According to these considerations, the catalytic activity is primarily an intrinsic property of Au nanoclusters. The influence of the support material is mainly indirect, via the shape and size of Au particles.[12] The difference between the bulk inert Au and the active nanoparticles is the relative number of undercoordinated atoms. It has been shown that the dependence of the catalytic activity on the cluster size is well correlated with the average coordination number of Au atoms in the cluster.[10] Nørskov and Hammer proposed the so-called "*d*-band model" to explain the trends in the catalytic activities of the metal surfaces, films, and clusters.[2] According to this model, adsorbate energy levels interact with the metal's *d* band to produce bonding and antibonding states. The position of the *d*-band center influences strength of the interaction and the occupancy of the resulting states, which are directly related to the potential barrier for adsorption as well as the adsorption energy. For bulk Au, the *d* band lies relatively deep below the Fermi level ($E_F$) and as a result the antibonding state is thought to be filled, making the interaction between the adsorbate and bulk Au repulsive. According to theoretical predictions, with the reduction of the cluster size and increasing the relative number of undercoordinated atoms, the *d* band tends to move closer to $E_F$.[9,13,14] Below a certain cluster size the antibonding state becomes higher than $E_F$, reducing the potential barriers for adsorption and dissociation. Indeed, the calculations of Phala and van Steen[14] show that the *d*-band center moves ~1 eV toward $E_F$ for 1.5-nm Au nanoclusters compared to that of the bulk. Although there is some criticism of the *d*-band model due to inconsistency of some of the predicted and calculated trends with experimental observations,[15] it is clear that an understanding of the changes occurring in the *d*-band structure with reduction of the cluster size is very important for revealing the origins of the emerging catalytic activity of gold nanoclusters. There are a plenty of theoretical reports on this topic, however, there are a few systematic experimental studies[16–18] on the *d*-band structure of Au nanoclusters.

In the present study, we prepared Au nanoclusters grown on amorphous carbon (*a*-C) substrates by molecular-beam epitaxy (MBE) and analyzed the properties of the *d* band by photoelectron spectroscopy (PES) using synchrotron-radiation (SR) light. The average size and shape of the clusters was estimated by high-resolution medium energy ion scattering spectroscopy (MEIS) and transmission electron microscopy (TEM). We determined *d*-band width ($W_d$) as well as an apparent $5d_{3/2}$-$d_{5/2}$ spin-orbit (SO) splitting ($E_{SO}$), and *d*-band center position ($E_d$) as a function of the number of Au atoms per cluster ($n_A$), and average coordination number ($n_C$) in a wide range ($11 < n_A < 1600$).

 

## II. EXPERIMENTAL DETAILS

We chose *a*-C as a support for Au nanoclusters for two reasons. First, Au bounds weakly to carbon, meaning that interaction with the support does not change the *d*-band structure of Au nanoclusters. Second, *a*-C gives a relatively weak, smooth, and featureless valence-band spectrum, which makes it easy to subtract the support contribution from the measured valence-band spectra. The *a*-C layers with a thickness of 10 nm were deposited on NaCl(001), KCl(001), LiF(001), and Si(001) substrates by cathodic-arc discharge. We have chosen the alkali-halide substrates to be able to observe Au nanoclusters on *a*-C by TEM, because the alkali-halide substrates can be dissolved in water, leaving a thin Au/*a*-C layer on the surface. However, an occasional charge up effect during photoemission made a spectral analysis to be complicated. In order to suppress the charge up effect, we deposited Au on the *a*-C/Si(001) substrates. Note that almost the same *a*-C layers are grown on alkali halides and Si(001) substrates, and thus the size and shape of Au nanoclusters are essentially the same for all substrates.

Au deposition and all measurements were performed *in situ* at a beamline 8 named SORIS at Ritsumeikan University SR Center. The beamline consists of three modules: (i) PES module, (ii) MEIS module, and (iii) a sample preparation chamber. Au nanoclusters have been grown by MBE at deposition rates of 0.1–0.3 ML/min [1 ML $= 1.39 \times 10^{15}$ atoms/cm$^2$ corresponding to the areal density of Au(111)].

The sizes and shapes of Au nanoclusters were estimated by high-resolution MEIS using a toroidal electrostatic analyzer employing 120-keV $He^+$ ions. After PES and MEIS measurements, the samples were taken to the ambient and transferred to TEM. The method for analyzing the cluster's size and shape by MEIS was described elsewhere.[19] The stopping power of the Au and $He^+$ fractions were measured in advance for Au thin layers stacked on a slightly oxidized Si(111) substrate. We employed the Lindhard-Scharff formula[20] for energy struggling and an exponentially modified Gaussian line shape in the MEIS analysis.[21]

Two types of varied space plane gratings in PES equipment cover photon energies from 20 eV up to 500 eV. We used photons with an energy of 60 and 80 eV for valence-band measurements and 140 eV for core-level Au 4*f* spectra. We calibrated the incident photon energy and determined a spectrometer work function using primary and secondary harmonic waves for the Au 4*f* core levels (assuming the binding energy of Au $4f_{7/2}$ to be 84.0 eV) and a Fermi-edge intensity cutoff for the valence band measured on standard polycrystal Au foil. The energy resolution of a hemispherical electrostatic analyzer at a pass energy of 2.9 eV was estimated to be ±0.05 eV.

The valence-band spectra analysis was performed in the following way. First, the measured spectra, shown in Fig. 1(a) for 0.3-ML Au coverage with black circles, were smoothed, and an inelastic background was subtracted as described in the original work by Shirley.[22] Figure 1(b) shows the resulting spectrum together with that from *a*-C which was measured in advance. Each spectrum was normalized by an integrated incident photocurrent. The difference spectrum, which is shown in Fig. 1(c), corresponds to the valence band from

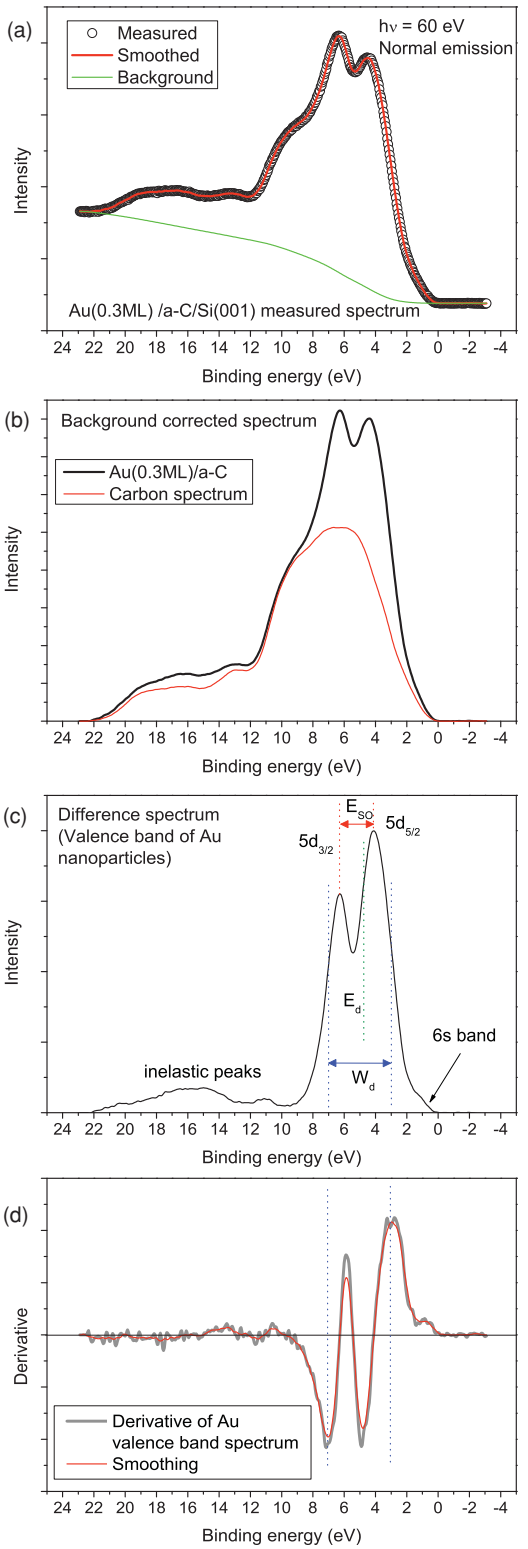


FIG. 1. (Color online) Au nanoclusters valence-band spectra analysis. (a) Measured spectrum of 0.3-ML Au deposited on *a*-C/Si(001). The spectrum was smoothed and the Shirley background was subtracted. (b) Background-corrected spectrum of Au(0.3ML)/*a*-C/Si(001) and a carbon substrate contribution. (c) The difference spectrum representing Au nanoclusters' valence band. The *d*-band parameters $W_d$, $E_{SO}$, and $E_d$ of Au nanoclusters are shown. (d) The derivative of the (c) spectrum and smoothed curve are used to find the points of inflections as boundaries of the *d* band.

Au nanoclusters. There are several methods to determine the width of the $d$ band: (i) using full width at half maximum (FWHM) parameters,[22,23] (ii) using onset and offset points of the $d$-band intensity, and (iii) using points of inflection as boundaries for the $d$ band.[24] Method (i) is not very reliable as we also have intensity contributions from the Au 6$s$ band and inelastically scattered electrons. Method (ii) is also difficult to apply, especially at a lower coverage, because of a smooth and continuous transition between the $d$-band intensity and the rest of the spectrum. We adopted the third method as the most reliable because the $d$-band intensity is relatively high and change much faster than the intensity of the $sp$ band or loss peaks, making the position of the points of inflection almost insensitive to the contribution of other parts of the spectra. To find the points of inflection, the spectra were differentiated and smoothed aggressively to reduce noise [see Fig. 1(d)]. The apparent Au $d_{3/2}$-$d_{5/2}$ SO splitting, $E_{SO}$, was determined as the difference in the peak positions of the Au $d$-band spectra. The $d$-band center, $E_d$, was obtained by calculating a middle point of an integral of the spectra between the inflection points.

We should also comment on concerns about possible angular and photon-energy dependencies of the $d$-band shape in PES spectra. All our PES experiments were performed using the photon energies of 60 eV (for the alkali-halide substrates) and 80 eV (for the Si substrates) and 140 eV for Au 4$f$ core-level spectra. The energy-dependent difference, if any, in the $d$-band parameters measured for all our samples lies within the error limits. We also used the same geometry (normal emission) for all the measurements. Therefore, the possible angular dependence may only come from the orientation of the clusters varied with size. The Au clusters were grown on amorphous carbon substrates and thus have a random in-plane orientation, although some preferential orientation in a vertical direction cannot be excluded. However, for larger clusters it is unlikely to grow with the preferential orientation varying with the size, and for smaller clusters the $d$-band shape is not very sensitive to the momentum of electrons, as shown in Ref. 16.

## III. RESULTS AND DISCUSSION

### A. Cluster size and average coordination number

The average size and its dispersion for Au nanoclusters were determined by high-resolution MEIS. Figure 2(a) shows a typical example of the MEIS spectrum measured for Au(0.05 ML)/$a$-C. It was already demonstrated that the shape of Au nanoclusters on oxides and sputtered highly-oriented pyrolytic graphite (HOPG) substrates is well approximated by a partial sphere with average diameter $d$, height $h$, and size dispersion $\sigma$.[19] The best-fit spectrum was obtained assuming a bimodal size distribution of Au clusters, which includes a smaller size group $G_S$ ($d = 0.9$ nm, $h = 0.45$ nm, $\sigma = 25\%$), and a larger group $G_L$ ($d = 3.0$ nm, $h = 1.5$ nm, $\sigma = 25\%$), and a volume ratio, $G_L/G_S$, of ~0.3. This means that the size distribution is asymmetric and for example, an asymmetric Gaussian and Lorentzian profile may also give a good fit. It must be noted also that the $G_L/G_S$ volume ratio of ~0.3 corresponds to the areal occupation ratio of 0.09. In PES measurements the kinetic energies of photoelectrons were 30–60 eV, which corresponds to a mean escape depth of

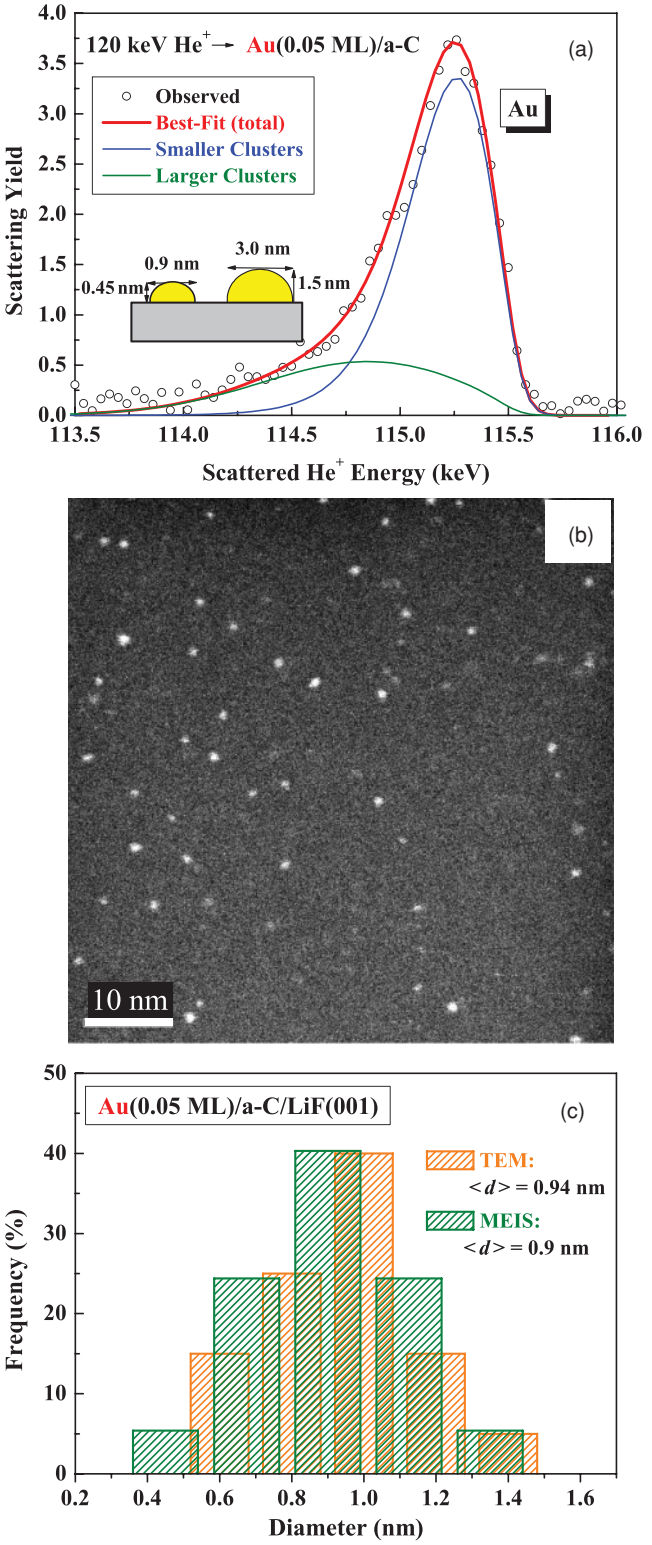


FIG. 2. (Color online) (a) MEIS spectrum observed for 120-keV $He^+$ ions incident on Au(0.05 ML)/$a$-C/NaCl. Incident and detection angles are $-45°$ and $45°$ with respect to the surface normal. The best-fit (red curve) was obtained assuming a bimodal size distribution with the $G_S$ group: $d = 0.9$ nm, $h = 0.45$ nm, $\sigma = 25\%$; and $G_L$: $d = 3.0$ nm, $h = 1.5$ nm, $\sigma = 25\%$. Volume and areal occupation ratios ($G_L/G_S$) are 0.3 and 0.09, respectively. (b) TEM image for Au(0.05 ML)/$a$-C. (c) A histogram of diameter distributions obtained by MEIS (green) and TEM (orange).

TABLE I. The size of Au nanoclusters determined by MEIS, the average number of Au atoms per cluster ($n_A$) calculated assuming a bulk Au number density, and the average Au coordination numbers ($n_C$) estimated from Eq. (1) proposed by Pirkkalainen and Serimaa (Ref. 25).

| Coverage (ML) | Diameter $d \pm 0.1$ (nm) | Height $h \pm 0.1$ (nm) | Volume (nm$^3$) | $n_A$ | $n_C$ |
|---|---|---|---|---|---|
| 0.05 | 0.9 | 0.45 | $0.19 \pm 0.13$ | $11.3 \pm 7.0$ | $6.3 \pm 0.6$ |
| 0.1 | 1.1 | 0.55 | $0.35 \pm 0.19$ | $20.6 \pm 11.2$ | $7.3 \pm 0.4$ |
| 0.2 | 1.4 | 0.7 | $0.72 \pm 0.30$ | $42.4 \pm 18.1$ | $8.3 \pm 0.3$ |
| 0.3 | 1.8 | 0.75 | $1.15 \pm 0.42$ | $67.8 \pm 25.0$ | $9.1 \pm 0.2$ |
| 0.4 | 2.2 | 0.8 | $1.74 \pm 0.55$ | $103 \pm 32$ | $9.7 \pm 0.1$ |
| 0.6 | 2.6 | 0.9 | $2.54 \pm 0.73$ | $150 \pm 43$ | $10.0 \pm 0.1$ |
| 0.7 | 2.7 | 0.95 | $2.93 \pm 0.80$ | $173 \pm 47$ | $10.1 \pm 0.1$ |
| 0.8 | 2.9 | 1.2 | $4.75 \pm 1.09$ | $280 \pm 64$ | $10.2 \pm 0.1$ |
| 1.0 | 3.05 | 1.7 | $8.70 \pm 1.62$ | $513 \pm 96$ | $10.3 \pm 0.05$ |
| 1.2 | 3.2 | 1.8 | $10.18 \pm 1.80$ | $600 \pm 106$ | $10.4 \pm 0.05$ |
| 1.5 | 3.65 | 2.0 | $14.6 \pm 2.29$ | $859 \pm 135$ | $10.7 \pm 0.03$ |
| 2.0 | 5.1 | 2.2 | $27.6 \pm 3.52$ | $1630 \pm 207$ | $11 \pm 0.03$ |

~0.5 nm. Due to this fact, the PES signal ratio from $G_L/G_S$ should be close to the areal occupation ratio, i.e., 0.09; thus, we neglect the contribution from $G_L$ in our analysis. We have also observed the Au cluster size distribution by TEM using the 300-keV electron beam to confirm our MEIS results [Fig. 2(b)]. The size distribution of $d$ (unfortunately the present TEM was unable to analyze the height of the clusters) determined by MEIS agrees with that observed by TEM as shown in Fig. 2(c) (only the size distribution of $G_S$ is indicated, as the $G_L$ group was omitted). The Au cluster sizes in a wide range of Au coverage are given in Table I.

The average number of atoms in each cluster ($n_A$) was calculated assuming a bulk atomic density of Au ($5.90 \times 10^{22}$ atoms/cm$^3$). Calculation of the average coordination number ($n_C$) is a nontrivial task, as it requires knowledge of the exact shape of the clusters. Recently, Pirkkalainen and Serimaa[25] proposed a simple formula to calculate the average coordination number for crystals of a spherical shape depending on their radius,

$$C_{\text{ave}} = (1 - y)C_{\infty} + yC_{\text{surf}}, \tag{1}$$

where $y \equiv 3t/r$, $C_{\text{ave}}$ is the average coordination number of atoms in a nanocluster, $C_{\infty}$ is the coordination number in a perfect bulk, $r$ is the radius of the particle in unit-cell dimensions, $C_{\text{surf}}$ is the average coordination number of surface atoms, and $t$ is a thickness of the surface layer in unit-cell dimensions (for the fcc lattice $C_{\infty} = 12$, $C_{\text{surf}} = 7.1808$, and $t = 0.4381$).[25] The formula is valid for spherical and hemispherical large clusters with good precision; however, the accuracy drops with decreasing cluster size due to shape deviations from the sphere (actual small crystalline clusters have a polyhedral shape). Nevertheless, the extended x-ray-adsorption fine structure (EXAFS) measurements[26] and density functional theory (DFT) calculations[27] for the average coordination numbers for small particles agree approximately with the values given by Eq. (1). The size distribution ($\sigma \approx 25\%$) of Au nanoclusters in our experiment will smooth out a discrepancy between the calculated and actual average coordination number even more. The $n_C$ values calculated using Eq. (1) for Au nanoclusters are also given in Table I.

### B. Photoemission spectra of the valence band and Au 4$f$ core levels

Figures 3(a) and 3(b) show the valence band and Au 4$f$ core-level spectra observed for Au/$a$-C at different Au coverages. The most obvious feature in the spectra is a shift of the $d$ band and Au 4$f$ core levels to a higher binding energy ($E_B$) side with decreasing coverage.

The shift of the spectral features to higher $E_B$ is reflected in Fig. 3(c), where the dependence of the $d$-band center and Au 4$f_{7/2}$ line positions on cluster size are given. Although the absolute values of the shift of the $d$-band center and 4$f$ core line differ, their overall behavior is correlated. One may also see that the apparent Fermi-edge onset of the valence-band structure in Fig. 3(a) is smeared and shifted with decreasing cluster size. All these facts support the idea that the observed shifts are due to the final-state effects. Other $d$-band parameters ($W_d$, $E_{\text{SO}}$) of the originally measured spectra are shown in Figs. 5(b) and 5(c).

The energy of photoelectrons from the valence band as well as core levels depends on the actual electronic structure of a solid (the initial-state effect) and that is also seriously affected by final-state effects. Our concern is, of course, the dependence of the actual electronic structure of Au nanoclusters on the particle size, that is, the initial-state effect. Therefore, the final-state effect contribution, which is also dependent on cluster size, should be removed from the data, if possible, as it is not related to the catalytic properties of Au nanoclusters. The final-state effects are referred to a series of phenomena related to extraction of a photoelectron from an atom, that is, relaxation of the electronic structure, conduction electron screening effects, and the electrostatic Coulomb interaction between the photoelectron and photohole.[28–33]There is still no consensus among the researchers studying metallic clusters by the photoemission technique on what is the main contribution to the observed valence band and core-level peak shifts. There are some consistent data, however, showing that the dependence of final-state relaxation and screening terms on the cluster size is quite small for a weakly interacting substrate such as carbon,[34,35] which was used in our experiments. In the present case, the contribution from the electrostatic Coulomb interaction, the so-called dynamic final-state effect,

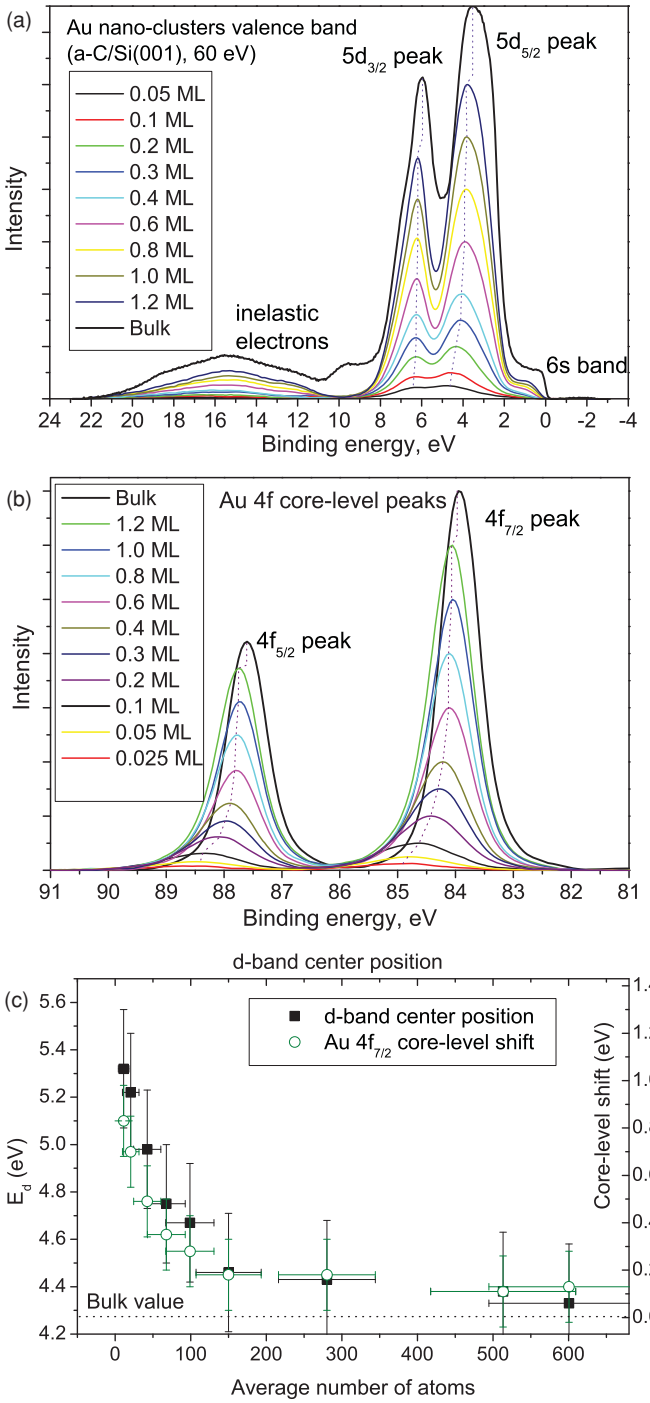


FIG. 3. (Color online) (a) The valence-band spectra of Au nanoclusters (measured at $h\nu = 60$ eV) at different coverage (after a substrate contribution subtraction). The dashed line guides the eye to indicate the shifts of $d_{3/2}$ and $d_{5/2}$ peaks to higher binding energies. The bulk polycrystal Au valence band is also shown for the reference. (b) The Au $4f$ core-level spectra of Au nanoclusters (measured at $h\nu = 140$ eV) at different coverages. The dashed line guides the eye, showing the shift of Au $4f_{5/2}$ and $4f_{7/2}$ lines to the higher binding energies. The bulk polycrystal Au core-level spectrum is also shown for the reference. (c) Derived position of the $d$-band center and shift of the Au $4f_{7/2}$ core line depending on the cluster size.

which comes from an electrostatic interaction between an emitted photoelectron and a positively charged cluster, may

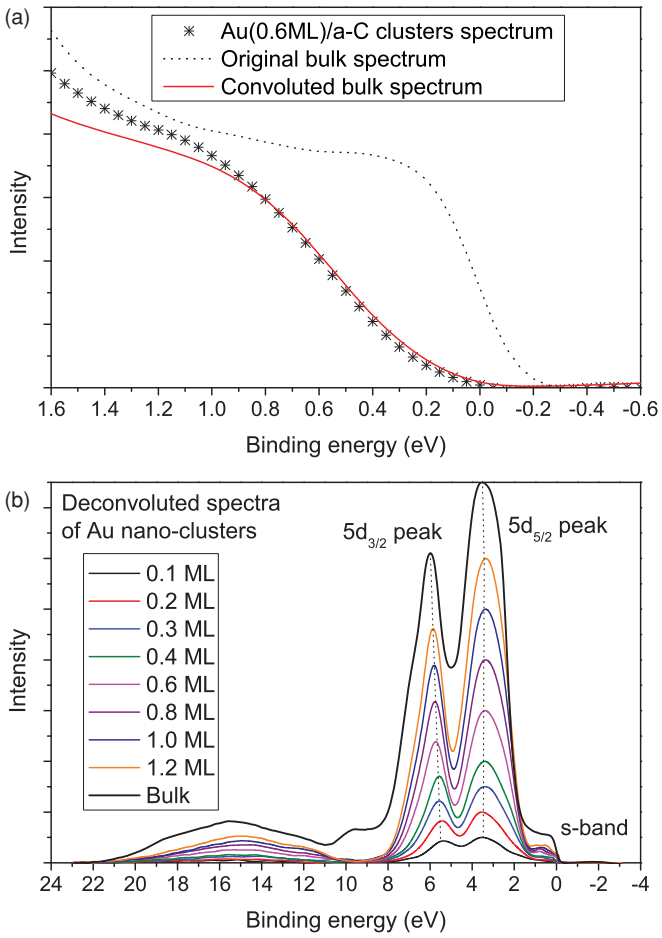


FIG. 4. (Color online) (a) An example of fitting of the convoluted Fermi-edge spectrum of the bulk Au to the valence-band spectrum of Au (0.6 ML) nanoclusters ($\tau = 0.5$ ps, $R_{\text{ave}} = 0.85$ nm, $\sigma = 0.25$). (b) Deconvoluted valence-band spectra of Au nanoclusters.

be very pronounced. This attractive interaction results in higher $E_B$ shifts. The photohole is neutralized within a finite time via tunneling of electrons from the substrate into a metal cluster.[36] The tunneling has a statistical nature with a probability $P(t)dt = (1/\tau)\exp(t/\tau)dt$, where $\tau$ is a relaxation time. Kinetic energy loss, $W$, of the photoelectrons can be expressed by the following probability distribution function,

$$P(W)dW = \frac{CW_{\max}}{(W_{\max} - W)^2} \exp\left(-\frac{CW}{W_{\max} - W}\right)dW, \quad (2)$$

where $C \equiv R/v\tau$, $v$ is a velocity of photoelectron, $W_{\max} = \alpha e^2/(4\pi\varepsilon_0 R)$ is a maximum kinetic energy loss, and $\alpha e$ ($\alpha \approx 0.5$ for Au) is an effective charge of the photohole. The equation assumes that Au clusters are spherical with a radius $R$ and the charge is located at the center of the sphere. There are several works in which this formalism was used successfully to fit the core-level shifts and the Fermi-edge onset of gold and silver nanoparticles depending on the radius of the nanoparticle.[37,38] We also apply this expression to estimate the final-state effect contribution to the $d$-band center shift.

As shown in Fig. 3(a), the apparent Fermi edge of the valence-band spectra moves to the higher binding energy with decreasing cluster size. From the shifts of the apparent Fermi

edge, its shape, and also from Au $4f$ core-level shifts, we may estimate the relaxation time $\tau$ and the effective radius of the clusters. Note that the shape of Au clusters grown on $a$-C is not a sphere, but almost a hemisphere, and the effective radius in this case should be close to the cluster height (for the normal emission). The reference spectrum near $E_F$ and the core-level spectrum have been taken from the bulk polycrystal Au foil. These spectra were convoluted using the kinetic energy loss distribution function [Eq. (2)] and also accounting for the cluster size distribution as follows:

$$S_{\text{final}}(E) = [G(R_{\text{ave}},\sigma)\otimes P(W,\tau,R)]\otimes S_{\text{bulk}}(E), \qquad (3)$$

where $S_{\text{bulk}}(E)$ and $S_{\text{final}}(E)$ are the bulk and convoluted spectra, respectively, $P(W,\tau,R)$ is the energy-loss distribution for clusters with radius $R$ [Eq. (2)], and $G(R_{\text{ave}},\sigma)$ is a Gaussian size distribution function for clusters with an average radius $R_{\text{ave}}$ and a size dispersion $\sigma$. By best fitting the convoluted bulk spectra to the observed ones near the Fermi edge for Au clusters, we found $\tau = 0.50 \pm 0.15$ ps, effective average radii $R_{\text{ave}} \approx h$, and $\sigma = 0.2$–$0.25$. We must note that $\tau$ is independent of the cluster size because it depends only on a tunneling probability of electrons from the support to the clusters. A typical example of the best fit of the Fermi edge is shown in Fig. 4(a). Using the same parameters for $\tau$, $R_{\text{ave}}$, and $\sigma$ for respective coverage we could also fit well the Au $4f_{7/2}$ core-level spectra (not shown here for brevity), although some corrections of the peak positions (0.2–0.3 eV to lower $E_B$) had to be made for smaller clusters to account for the increase of the surface-related component compared to the bulk contribution [the reported $E_B$ difference between the surface and bulk components of Au $4f$ peaks is 0.2–0.4 eV (Refs. 39,40)]. After determination of the fitting parameters, the corresponding $d$-band spectrum which reflects the initial state was obtained by deconvolution using the modified Gold's method.[41] The result is shown in Fig. 4(b). One can see that the Fermi-edge positions of the deconvoluted spectra are now coincide with the bulk value. Dotted lines in Fig. 4(b) indicate the positions of the $d$-band peaks, $d_{3/2}$ and $d_{5/2}$. The $d_{5/2}$ peak position stays almost constant, while the $d_{3/2}$ peak moves slightly toward lower $E_B$ ($\sim$0.45 eV for change in the size from 600 to 20 atoms/cluster).

The $d$-band parameters, $W_d$, $E_{\text{SO}}$, and $E_d$, derived from the original and deconvoluted data, are given in Fig. 5 as a function of $n_A$. It is clear from the spectra that the parameters of the $d$ band are almost constant for larger clusters and start to change dramatically for $n_A$ below $\sim$150 atoms/cluster. This critical size corresponds to a diameter of $\sim$2.6 nm of Au clusters with the shape of a partial sphere (close to a hemisphere). The $d$-band width, $W_d$, drops from a value of 4.2–4.5 eV, which is close to the bulk one, to 3.4 eV with decreasing cluster size. The apparent $5d_{3/2}$-$d_{5/2}$ SO splitting, $E_{\text{SO}}$, is also reduced by $\sim$1 eV from a bulk value of 2.55 eV and reaches approximately the atomic value of 1.52 eV for the smallest clusters with $n_A \approx 11$. The results obtained here for $W_d$ and $E_{\text{SO}}$ reflect band narrowing and reduction of the $d$-orbital overlap which are caused by hybridization of a smaller number of wave functions of valence electrons for smaller clusters. The apparent SO splitting is a result of an atomic SO splitting and the so-called "banding interaction" caused by the interaction of the $d$-orbitals of neighboring Au atoms, and thus depends strongly on the number of nearest neighbors, i.e., the coordination number.[24,42] Reduction of the apparent SO to almost the atomic value clearly shows

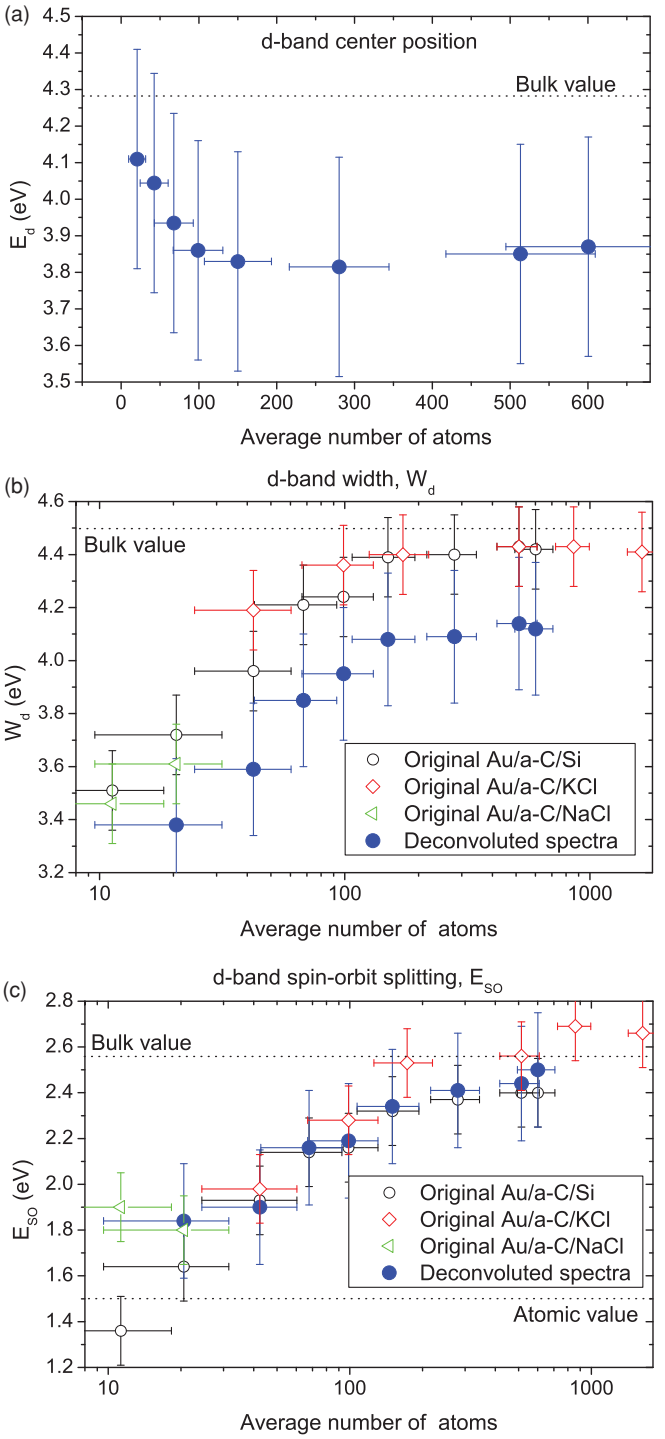


FIG. 5. (Color online) (a) The $d$-band center derived from the deconvoluted spectra of Au nanoclusters. (b) The comparison between the $d$-band width, $W_d$, measured before (open symbols) and after (filled circles) deconvolution of the spectra. (c) The comparison between the apparent $d$-band spin-orbit splitting $E_{\text{SO}}$ measured before (open symbols) and after (filled circles) deconvolution of the spectra. The $n_A$ values is given in logarithmic scale for the latter two plots to improve data readability.

a significant reduction of the coordination number for smaller clusters. The shift of the $d$ band as a whole is represented by the $d$-band center position as plotted in Fig. 5(a). Although the shift of the $d$ band is diminished considerably as compared with that before the deconvolution treatment [see Fig. 3(c)], still, for cluster sizes below ∼150 atoms/cluster, the $d$-band center, $E_d$, moves rapidly to higher $E_B$ values. This result is unexpected because it contradicts the $d$-band theory[9,13,14] and recent theoretical calculations, which stated that the $d$ band moves closer to the Fermi level with decreasing cluster size. Interestingly, however, all the $d$-band center positions derived from the deconvoluted spectra for Au nanoclusters take lower $E_B$ values than that for the bulk Au. This means that a reduction in a potential barrier for molecular adsorption and dissociation for Au nanoclusters as compared to that for the bulk Au may be indeed caused by, to some extent, the $d$-band shifting toward $E_F$. However, the value of the shift is much smaller than the predicted one (up to 1 eV according to Ref. 14), and a dependence on the cluster size contradicts a widely accepted theoretical consideration of monotonous movement of the $d$-band center toward $E_F$ with decreasing cluster size.

One of the possible explanations for this contradiction is contraction of the Au-Au bond in real nanoclusters with size reduction. DFT calculations,[27] and EXAFS measurements[43] show that the Au-Au bond length is reduced by almost 5% for clusters with a diameter of ∼1 nm as compared with the bulk Au. This may increase an overlap integral for the $d$ orbitals and push the $d$ band to higher $E_B$ values. In the EXAFS experiments[43] a significant reduction of the distance starts when the average coordination number of Au atoms drops below 10. In our experiments this corresponds to clusters containing ∼150 atoms. Indeed, we observe movement of the $d$-band center to higher binding energies staring below ∼150 atoms. We have tried to get some supportive information for the above proposal by calculating the $d$-band structure of small Au clusters based on the *ab initio* DFT method using the VASP code.[44,45] Trial clusters were assumed to take a simple cuboctahedral $Au_{19}$, $Au_{38}$, and $Au_{55}$ form (similar to those in Ref. 27). The local density approximation (LDA) approximation has been used because it gives the equilibrium unit-cell parameter of 4.06 Å, which is in better agreement with the experimental value of 4.08 Å rather than that obtained by the generalized gradient approximation (GGA). Cluster geometries were relaxed until the forces acting on atoms became smaller than 0.01 eV/Å. As a result, all three clusters show inward relaxation of the outermost Au atoms, namely, contracting the Au-Au bond from the bulk value of 2.87 Å down to ≈2.67 Å depending on the location of the outer atoms. The average contraction of the Au-Au bond was ∼3% for $Au_{38}$ and $Au_{55}$ and ∼4% for $Au_{19}$. All three relaxed clusters show movement of the $d$-band center to a higher $E_B$ as compared to the unrelaxed geometry. We also performed the calculations in which we manually and uniformly contracted the Au-Au interatomic distance for a fixed $Au_{38}$ cluster, varying it from 0.98 down to 0.88 of that of the bulk distance with a decrement of 0.2. As a result, we obtained a monotonous and almost linear shift of the $d$-band center to higher $E_B$ with decreasing interatomic distance. Reduction of 4%–5% for the Au-Au bond length leads to the $E_d$ shift of 0.4 eV away from $E_F$ as compared to that for the noncontracted cluster. It is also noteworthy that the present results for $E_d$ dependence on the cluster size are quite consistent with those observed for Au overlayers on Ru(001) substrate,[24] where a similar shift of $E_d$ to higher $E_B$ has been observed with decreasing Au coverage. As the metallic radius of Au is larger than that of Ru atoms, the first pseudomorphic overlayers of Au experience a compressive stress, which results in contraction of Au-Au distance [lattice mismatch between Au(111) and hexagonal Ru(001) is 4%–5%].All these facts support our hypothesis of $d$-band movement away from $E_F$ due to the Au-Au bond contraction.

It is important to see other experimental data reported so far to compare with our results. There are several important works studying electronic properties of Au nanoclusters.[16,17] However, apart from our primary interests, these reports only address the $d$-band splitting without the $d$-band center position and the $d$-band width. Actually, our data on $E_{SO}$ agree well with the results obtained in these works. On the other hand, the analysis of the $d$ band, similar to ours, was performed by Bzowski *et al.*[24] for Au thin films on Ru(001). Their

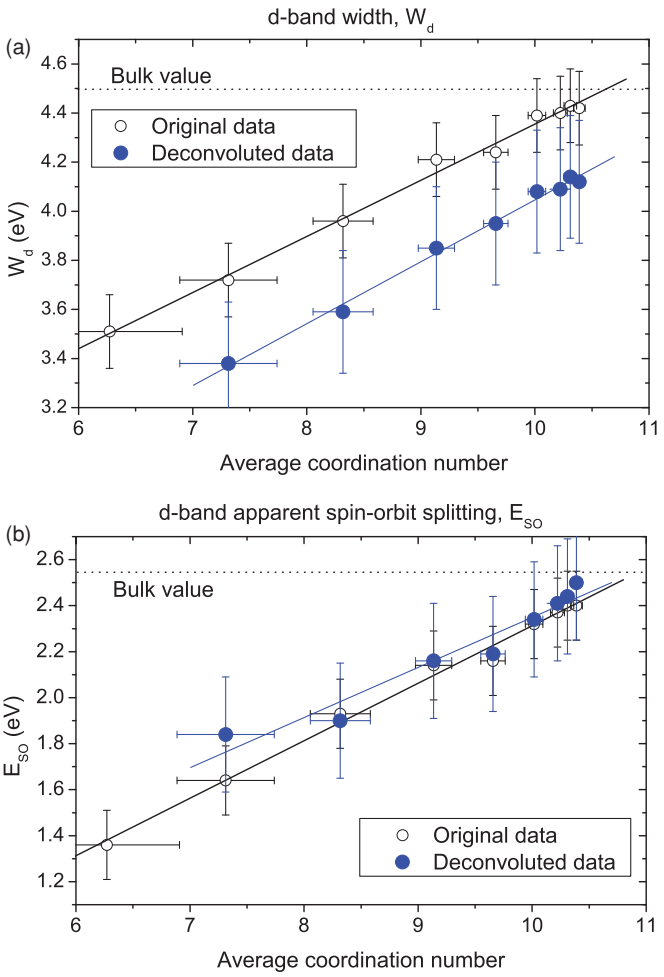


FIG. 6. (Color online) (a) The $d$-band width ($W_d$) and (b) the apparent $d$-band spin-orbit splitting ($E_{SO}$) depending on the average coordination number of Au atoms in gold nanoclusters. The open circles represent the original measured data, and filled circles correspond to the data after deconvolution treatment.

results are well consistent with our data obtained here for Au nanoclusters. They found *d*-band narrowing and a *d*-band center that shifts apart from $E_F$ with decreasing Au coverage. In their study, however, the *d*-band parameters change almost linearly with Au coverage. It is easy to explain this result if we assume that the coordination number of Au atoms plays an important role. The layer-by-layer growth of Au film on Ru(001) means that the number of undercoordinated Au atoms on the surface is almost constant, whereas the number of fully coordinated atoms in inner layers is growing linearly with increasing coverage. The average Au coordination number should change, therefore, almost linearly, resulting in the linear dependence of the *d*-band parameters on Au coverage. In the case of nanoclusters, the average coordination number cannot be expressed by a linear function of the coverage and the cluster size. Indeed, we obtain the linear dependence of the *d*-band parameters upon the average coordination number of Au atoms calculated using Eq. (1), as indicated in Fig. 6.

We emphasize again that all the *d*-band parameters change dramatically below a critical $n_A$ value of ∼150 atoms/cluster. This critical size coincides well with the onset for abrupt reduction of the average coordination number and contraction of Au-Au bond length, and also with the onset for emerging catalytic activity of Au nanoclusters reported so far.[46,47]

## IV. CONCLUSIONS

We have studied systematically the *d*-band parameters for Au nanoclusters on *a*-C in a wide range of cluster sizes ($11 < n_A < 1600$). The cluster size and shape, together with the size dispersion, were determined by high-resolution MEIS and TEM. Drastic changes take place for all the *d*-band parameters as well as for Au $4f$ core levels for $n_A \leqslant 150$ atoms/cluster corresponding to the cluster diameter of ∼2.6 nm. The values of the *d*-band width ($W_d$) and the apparent SO splitting ($E_{SO}$) decrease steeply below this critical size. This is a consequence of *d*-band narrowing caused by hybridization of a smaller number of wave functions of valence electrons for smaller clusters and of the reduction of the coordination number of Au atoms. The *d*-band center shifts apart from the Fermi level with decreasing cluster size. This is partly due to the dynamic final-state effect. We tried to derive the initial-state *d*-band spectra of Au nanoclusters by deconvolution treatment assuming a Gaussian cluster size distribution and the formalism of the dynamic final-state effect developed for spherical particles.[36] The deconvoluted data show that the $E_d$ position is closer to the $E_F$ as compared to the bulk value, however, it still tends to move away from $E_F$ with decreasing Au nanocluster size. Such a behavior is ascribed to the contraction of average Au-Au bond length with decreasing the cluster size. This trend was evidenced by the *ab initio* calculations. There are some uncertainties included in the deconvolution processing related to both the mathematical procedure itself as well as a physical understanding. For example, for the smallest clusters, a metal-insulator transition may take place and a band gap may open. This may overestimate the contribution from the dynamic final-state effect. In spite of these difficulties, we believe that the present results provide a prominent insight into the dramatic changes of the *d*-band parameters of Au nanoclusters and provide a critical approach to the *d*-band model application. It is also found that the *d*-band parameters such as width and apparent SO splitting are scaled almost linearly with the average coordination number $n_C$, indicating the importance of the number of undercoordinated atoms in the clusters. It is noteworthy that the present data of the *d*-band parameters for Au nanoclusters are quite consistent with those measured for Au overlayers on Ru(001).[24] The behavior of the *d* band moving away from $E_F$ observed for thin Au layers and small clusters with decreasing Au coverage and cluster size can be explained by the contraction of the Au-Au bond length, suggesting the importance of strain upon the *d*-band structures of thin metal films and clusters.

## ACKNOWLEDGMENTS

The authors would like to thank M. Kohyama for useful comments on the *d*-band structure. Special thanks are also due to our colleagues, H. Okumura and H. Yamada, for help in the experiment. This work was supported partly by Japan Science and Technology Agency, JST, CREST, and also by the Ministry of Education, Culture, Sports, Science and Technology, MEXT, Japan.

*anton@fc.ritsumei.ac.jp

[1] R. Paddephatt, *The Chemistry of Gold* (Elsevier, New York, 1978).
[2] B. Hammer and J. Nørskov, Nature (London) **376**, 238 (1995).
[3] M. Haruta, N. Yamada, T. Kobayashi, and S. Iijima, J. Catal. **115**, 301 (1989).
[4] M. Haruta, Catal. Today **36**, 153 (1997).
[5] M. Valden, X. Lai, and D. Goodman, Science **281**, 1647 (1998).
[6] J. G. Wang and B. Hammer, Phys. Rev. Lett. **97**, 136107 (2006).
[7] A. Sanchez, S. Abbet, U. Heiz, W.-D. Schneider, H. Häkkinen, R. N. Barnett, and U. Landman, J. Phys. Chem. A **103**, 9573 (1999).
[8] Y. Xu and M. Mavrikakis, J. Phys. Chem. B **107**, 9298 (2003).
[9] N. Lopez, T. Janssens, B. Clausen, Y. Xu, M. Mavrikakis, T. Bligaard, and J. Nørskov, J. Catal. **223**, 232 (2004).
[10] B. Hvolbæk, T. Janssens, B. Clausen, H. Falsig, C. Christensen, and J. K. Nørskov, NanoToday **2**, 14 (2007).
[11] G. Mills, M. Gordon, and H. Metiu, J. Chem. Phys. **118**, 4198 (2003).
[12] T. Janssens, A. Carlsson, A. Puig-Molina, and B. Clausen, J. Catal. **240**, 108 (2006).
[13] T. Jiang, D. Mowbray, S. Dobrin, H. Falsig, B. Hvolbæk, T. Bligaard, and J. K. Nørskov, J. Phys. Chem. C **113**, 10548 (2009).
[14] N. Phala and E. van Steen, Gold Bull. **40**, 150 (2007).
[15] C. Lu, I. Lee, R. Masel, A. Wieckowski, and C. Rice, J. Phys. Chem. A **106**, 3084 (2002).
[16] S.-T. Lee, G. Apai, M. G. Mason, R. Benbow, and Z. Hurych, Phys. Rev. B **23**, 505 (1981).
[17] H. Kröger, P. Reinke, M. Müttner, and P. Oelhafen, J. Chem. Phys. **123**, 114706 (2005).
[18] K. Taylor, C. Pettiette-Hall, O. Cheshnovsky, and R. Smalley, J. Chem. Phys. **96**, 3319 (1992).

[19] A. Iwamoto, T. Okazawa, T. Akita, I. Vickridge, and Y. Kido, Nucl. Instrum. Methods B **266**, 965 (2008).
[20] J. Lindhard, and M. Scharff, Kgl. Den. Vidensk. Selsk. Mat. Fys. Medd. **27**, 15 (1953).
[21] M. Hazama, Y. Kitsudo, T. Nishimura, Y. Hoshino, P. L. Grande, G. Schiwietz, and Y. Kido, Phys. Rev. B **78**, 193402 (2008).
[22] D. Shirley, Phys. Rev. B **5**, 4709 (1972).
[23] G. K. Wertheim, D. N. E. Buchanan, and V. Lee, Phys. Rev. B **34**, 6869 (1986).
[24] A. Bzowski, T. K. Sham, R. E. Watson, and M. Weinert, Phys. Rev. B **51**, 9979 (1995).
[25] K. Pirkkalainen and R. Serimaa, J. Appl. Crystallogr. **42**, 442 (2009).
[26] R. Benfield, J. Chem. Soc., Faraday Trans. **88**, 1107 (1992).
[27] O. Häberlen, S. Chung, M. Stener, and N. Rösch, J. Chem. Phys. **106**, 5189 (1997).
[28] G. Moretti, J. Electron. Spectrosc. **95**, 95 (1998).
[29] S. Kohiki, Appl. Surf. Sci. **25**, 81 (1986).
[30] G. Moretti and P. Porta, Surf. Sci. **287**, 1076 (1993).
[31] R. N. nez González, A. Reyes-Serrato, D. Galván, and A. Posada Amarillas, Comput. Mater. Sci. **49**, 15 (2010).
[32] M. Yoshiya, I. Tanaka, K. Kaneko, and H. Adachi, J. Phys Condens. Matter **11**, 3217 (1999).
[33] G. K. Wertheim and S. B. DiCenzo, Phys. Rev. B **37**, 844 (1988).
[34] D.-Q. Yang and E. Sacher, Appl. Surf. Sci. **195**, 187 (2002).
[35] M. G. Mason, Phys. Rev. B **27**, 748 (1983).
[36] H. Hövel, B. Grimm, M. Pollmann, and B. Reihl, Phys. Rev. Lett. **81**, 4608 (1998).
[37] A. Tanaka, Y. Takeda, T. Nagasawa, H. Sasaki, Y. Kuriyama, S. Suzuki, and S. Sato, Surf. Sci. **532**, 281 (2003).
[38] A. Tanaka, Y. Takeda, I. Imamura, and S. Sato, Appl. Surf. Sci. **237**, 537 (2004).
[39] P. Heimann, J. van der Veen, and D. Eastman, Solid State Commun. **38**, 595 (1981).
[40] A. Tanaka, Y. Takeda, T. Nagasawa, and K. Takahashi, Solid State Commun. **126**, 191 (2003).
[41] *Deconvolution of Images and Spectra*, ed., edited by P. Jansson (Academic, San Diego, 1997), pp. 114–116.
[42] G. Crecelius and G. Wertheim, Chem. Phys. Lett. **63**, 519 (1979).
[43] J. Miller, A. Kropf, Y. Zha, J. Regalbuto, L. Delannoy, C. Louis, E. Bus, and J. van Bokhoven, J. Catal. **240**, 222 (2006).
[44] G. Kresse and J. Furthmuller, Comput. Mater. Sci. **6**, 15 (1996).
[45] G. Kresse and J. Furthmuller, Phys. Rev. B **54**, 11169 (1996).
[46] M. Haruta, Chem. Record **3**, 75 (2003).
[47] T. Fujitani, I. Nakamura, T. Akita, M. Okumura, and M. Haruta, Angew. Chem. Int. Ed. **48**, 9515 (2009).